

This is a postprint version of the following published document:

Barrios, David; Vergaz, Ricardo; Sánchez-Pena, José M.; García-Cámara, Braulio; Granqvist, Claes G.; Niklasson, Gunnar A. (2015). Simulation of the thickness dependence of the optical properties of suspended particle devices. *Solar Energy Materials and Solar Cells*, v. 143, pp.: 613-622.

DOI: <https://doi.org/10.1016/j.solmat.2015.05.044>

© 2015 Elsevier B.V. All rights reserved.



This work is licensed under a [Creative Commons AttributionNonCommercialNoDerivatives 4.0 International License](https://creativecommons.org/licenses/by-nc-nd/4.0/)

Thickness dependence simulations of the optical properties for a suspended particle device derived from scattering and absorption coefficients

David Barrios ^{a, b, *}, Ricardo Vergaz ^b, Jose M. Sanchez-Pena ^b,
Braulio Garcia-Camara ^b, Claes G. Granqvist ^c, Gunnar A. Niklasson ^c
^a Facultad de Informática y Electrónica, Escuela Superior Politécnica de
Chimborazo, Riobamba, Ecuador

^b Grupo de Displays y Aplicaciones Fotónicas, Departamento de Tecnología
Electrónica, Universidad Carlos III de Madrid, C/Butarque 15, E-28911
Leganés, Madrid, Spain

^c Department of Engineering Sciences, The Angstrom Laboratory, Uppsala
University, P.O. Box 534, SE-75121 Uppsala, Sweden

Corresponding author: David Barrios

Universidad Carlos III de Madrid, Dept. Tecnología Electrónica, C/Butarque, 15,
E28911, Leganés, Madrid, Spain

Phone Number: (34) 91 624 8390, Fax Number (34) 91 624 94 30

E-mail: dbarrios@ing.uc3m.es

Abstract

Suspended particle devices (SPDs) constitute an electrically powered chromogenic technology, in which the active layer quickly switches from a bluish-black dark color to a clear grey color when an AC electric field is applied. Refractive index and extinction coefficients, in addition to scattering and absorption coefficients, were derived from four flux and two flux models. They were used in model calculations to predict the direct and the total (and hence the diffuse) components of the transmittance and the reflectance, together with the color appearance and the haze, as a function of thickness of the active layer. The optimum thickness for the SPDs performance can be determined in this way.

Keywords

Electro-optical materials; Optical properties; Organic materials; Electro-optical devices; Scattering, particles; Thin films, Optical properties; Solar energy.

1. Introduction

An electromagnetic radiation, such it is the solar radiation, can be reflected (R), scattered (S), absorbed (A) or transmitted (T), when it crosses a medium with different refractive index than the one from it travels. This relationship is known as the Kirchhoff's law applied to energy conservation ($R+A+S+T=1$), and the materials able to control any of these four parameters (by means of different external stimulus) are known as chromogenic materials, and one of their main applications are optically switchable smart windows. Optical characterization of these materials includes total and diffuse reflectance and transmittance measurements, which are carried out using an integrating sphere based spectrometer [Roo93]. The direct transmittance (T_{dir}) and the specular reflectance (R_{spec}) are computed by subtracting the total and the diffuse components, and stand for the R and T parameters in the previous relation. The sum of the diffuse transmittance and reflectance stands for the S parameter related to scattering ($S=T_{diff} + R_{diff}$). Absorption (A) parameter can be therefore derived by knowing R, T and S ($A=1-T-R-S$).

Electrophoretic SPD is one of the three main chromogenic technologies with external stimulus triggering signal commonly studied for smart windows applications, with chromic materials (electrochromic (EC) materials) and liquid crystals (LC) (polymer dispersed liquid crystals (PDLC), [Lam03]). The SPD technology uses the movement up and down of bluish-black colored absorption particles that are suspended in a cross linked polymer matrix in order to control light transmission, by applying an AC voltage signal (Fig. 1, [Bar12]).

A SPD consists of 3-5 layers. The active layer has millions of black needle shaped dipole particles of (dihydrocinchonidine bisulfate polyiodide) or heraphathite ($<1 \mu\text{m}$ long) suspended in a polymer. The particles are polyiodide (polyhalide crystals) [Cha02] and exhibit a large optical anisotropy, being heraphathite (quinine bisulphate polyiodide) [Kah09] used on polarizers and other optical devices of previous works [Kno09]. The optical anisotropy of heraphathite has been studied in detail in [LLi09]. Other related compounds have been used for SPDs [Tak97 and Sax03]. The size of the particles should be lower than 200 nm in order to minimize light scattering and avoid a non-desired haze effect. This layer is laminated between two dielectric layers, which are filled between two electrical conductors (such as ITO) and placed between two glass layers [Lam03]. In the off state the suspended particle (SP) droplets are randomly oriented, absorbing and scattering visible light. The SPD window shows a bluish-black

dark color since most of the light is not passing through the SPD film, and the scattering effect is mainly due to small particles, which is more effective at short wavelengths. When the electric field is applied, the particles line up and become perpendicular to the window, allowing more light crossing and hence increasing the transmission. Without memory effect, the electric field must be maintained for keeping the film transparent [Lam98].

The black, light absorbing suspended particles are the main responsible for extinction of the electromagnetic radiation field. Extinction is a process related to attenuation, since the radiant intensity decreases (while emission increases it). Extinction is due to absorption and scattering. Absorption is a process that removes the radiant energy from the electromagnetic field and transfers it to other forms of energy. Scattering is a process that does not remove energy from the radiation field but may redirect it. In previous works, the authors decoupled the extinction coefficients into scattering and absorption coefficients of a SPD sample by means of the two flux and four flux models [Bar13]. In this work, the study of the simulated optical appearance, and other parameters such as optical haze and contrast, was derived from the extensive scattering and absorption coefficients resulted from two flux model.

2. Experiments (Theory?)

As it was detailed in previous works [Bar13], the SPD investigated in this work has an active area of 28 x 22 cm² and a thickness of 300 μm. It is a CriRegulite device supplied by CRICURSA (Cristales Curvados S. A., Barcelona, Spain), which is a licensee of Research Frontiers, Inc. (Woodbury, NY, USA). The SPD was operated with a sinusoidal signal at 50 Hz and a peak voltage U between 0 and 100 V. Photographs and functioning principles of a SPD in “OFF” and “ON” states, with 0 and 100 V AC 50 Hz sinusoidal signal applied, respectively, are shown in Fig. 2.

The four-flux model includes 4 equations related to $T_{dir}=T_{cc}$, $R_{spec}=R_{cc}$, $T_{diff}=T_{cd}$ and $R_{diff}=R_{cd}$ [MLG84, MLG86 and Var98]. Collimated-collimated (cc) measurements (i.e., collimated measurements when illuminating with collimated light), including R_{spec} and T_{dir} , as well as collimated-diffuse (cd) measurements (i.e., diffuse measurements when illuminating with collimated light), including R_{diff} and T_{diff} of the SPD sample at both OFF and ON states, were measured using a double-beam spectrophotometer (Perkin-Elmer Lambda 900) equipped with an integrating sphere in the 300 to 2500 nm wavelength range (Fig. 3).

As shown in Fig. 4, four-flux model considers four light beams, two downwelling collimated and diffuse beams, i_c and i_d , and two upwelling collimated and diffuse beams, j_c and j_d . However, two-flux model considers only two light beams, both totals (with collimated and with diffuse part), one downwelling beam “i” and one upwelling beam “j”.

According to Körtum equations [Kor69] for front and back interfaces “1” and “2” respectively, the two cc equations of the four-flux model for T_{dir} and R_{spec} can be expressed as:

$$T_{cc} = T_{dir} = \frac{T_1^i \cdot T_2^i}{1 - R_1^j \cdot R_2^i} = \frac{(1 - r_c)^2 \cdot e^{-(\alpha+\beta)\delta}}{1 - r_c^2 \cdot e^{-2(\alpha+\beta)\delta}} \quad (\text{Eq.1})$$

$$R_{cc} = R_{spec} = R_1^i + \frac{T_1^i \cdot T_1^j \cdot R_2^i}{1 - R_1^j \cdot R_2^i} = r_c + \frac{(1 - r_c)^2 \cdot r_c \cdot e^{-2(\alpha+\beta)\delta}}{1 - r_c^2 \cdot e^{-2(\alpha+\beta)\delta}} \quad (\text{Eq.2})$$

Knowing that r_c is the collimated interface reflectance computed by Fresnel equations at normal incidence and assuming that the multilayer SPD structure is approximated as a single layer with a continuous refractive index over all its thickness, the collimated interface reflectance is obtained as:

$$r_c = \left(\frac{n_2 - n_1}{n_2 + n_1} \right)^2 = \left(\frac{n - 1}{n + 1} \right)^2$$

In four-flux cc equations, each parameter is identified as:

- $T_1^i = (1 - r_c)$ the transmittance of interface “1” with light beam “i” sense.
- $R_1^i = r_c$ the reflectance of interface “1” with light beam “i” sense.
- $T_2^i = (1 - r_c) \cdot e^{-(\alpha+\beta)\delta}$ the transmittance of interface “2” with light beam “i” sense.
- $R_2^i = r_c \cdot e^{-(\alpha+\beta)\delta}$ the reflectance of interface “2” with light beam “i” sense.
- $T_1^j = (1 - r_c) \cdot e^{-(\alpha+\beta)\delta}$ the transmittance of interface “1” with light beam “j” sense.

Since $\text{ext} = \alpha + \beta$ is the extinction coefficient due to both scattering and absorption, and the collimated interface reflectance r_c only depends on the real part of the refractive index n , cc four-flux equations 1 and 2 of the four-flux model consist of a system with two equations and two unknowns, extinction coefficients and real part of the refractive index (ext and n) which can be solved.

Now the problem is to decouple the extinction coefficients into the intrinsic absorption and scattering coefficients (α & β), which determination from experimental spectral transmittance and reflectance measurements in light scattering media is a difficult problem [Rod00]. Knowing the value of the separated coefficients of a film of

a determined thickness exhibiting R_{spec} and R_{diff} as well as T_{dir} and T_{diff} is a powerful tool in order to predict the value of these optical properties for different thicknesses of the same film. However, the other two four-flux cd equations include parameters such as forward scattering ratios (FSR), average crossing parameter (ACP) and diffuse interface reflectances for diffuse R_{diff} and T_{diff} components [Var98]. Since these diffuse equations include (α & β) parameters separately, decoupling extinction coefficient into scattering and absorption coefficients is a required task. However, inverting diffuse equations in order to obtain the value of these parameters from the experimental measurements seems a very difficult problem, being advanced fitting methods like the spectral projected gradient method the only option applied for such problem [Cur02].

Two flux models [MLG86] are another simpler but approximated option of determining the parameters associated to diffuse light, being the conditions of applicability studied in detail [Var97a, Var97b and Var99]. Levinson et al. considered that total components R_{tot} and T_{tot} can be determined by two flux models when the scattering is weak and R_{spec} and T_{dir} are close to the total R_{tot} and T_{tot} components respectively (which is traduced directly to a spectral value of ACP close to 1, as in non scattering media) [Lev05]. The process of determination and decoupling the extensive scattering and absorption coefficients (S & K) of the SPD sample consists on several steps, including the spectral interface reflectance to collimated light r_c obtained by a fitting process using four flux collimated equations, from which it can be derived the spectral refractive index n of the film, which is used for computing the spectral interface reflectance to diffuse light r_d , which together with the spectral diffuse fractions of light determined at the top and the bottom interfaces allow to obtain the spectral total interface reflectance also at the top and bottom interfaces of the SPD sample (being the top interface the closer to the spectrometer illuminant). Equations of two flux model are then used for total components once knowing the total interface reflectances. The change of the refractive index at each interface was taken into account by using the Saunderson correction. Finally, S & K are determined by a fitting process, once the values of these parameters have been previously obtained.

Extinction coefficients and refractive index were fitted by four- flux collimated-collimated (cc) equations. Decoupling extinction into scattering and absorption coefficients was derived by applying the Kubelka-Munk model and the Saunderson correction to the measured R_{tot} and T_{tot} in Fig. 5. Diffuse fractions of light at each

interface, refractive index and collimated and diffuse interface reflectances were computed as intermediate values.

Once S & K are obtained by the below detailed method, the predicted optical properties T_{dir} , T_{diff} , T_{tot} , R_{spec} , R_{diff} and R_{tot} were simulated for several thicknesses of the internal layer of the SPD sample different than the 300 μm of the film of the constructed device.

However, the two-flux model used in [Bar13] is only an approximation. For the measurements of transmittance and reflectance performed to the SPD sample by using the spectrometer Perkin Elmer Lambda 900 (available at the Angstrom Laboratory of Uppsala), the initially collimated light provided by the light source is diffused when crossing the SPD sample, being the scattering of the SPD not as strong to consider diffuse illumination. The phenomenological (also called extensive values) scattering and absorption coefficients (S & K) are properly calculated by the two flux KM model when all light in the film is perfectly diffuse, which is not the present case in the SPD sample. Hence in this case it should be necessary to apply the use of four-flux model, but equations of diffuse components include new unknown parameters, making more difficult to accurately find the values of the scattering and absorption coefficients. On the other hand, Maheu, Letoulouzan and Gouesbet (MLG) established in 1984 the formulas for transmittance and reflectances of a four flux model [MLG84] (two fluxes travelling in the forward direction and two fluxes travelling in the backward direction, being one collimated and one diffuse in each direction, Fig. 5-up). The scattering and absorption coefficients appearing in the MLG model (α & β) are non-phenomenological or also called intrinsic values. Four-flux model requires the introduction of two new parameters, the average path parameter or average crossing path parameter (ACP) and the forward scattering ratio (FSR).

It must be noted that, contrary to the equation of the reflectance, the equation of the transmittance was not originally proposed in the KM model, being possible to find in a later study of special cases of MLG [MLG86].

$$T = \frac{(1 - R_g) \cdot \tilde{b}}{\tilde{b} \cosh(\tilde{b} S \delta) + a - R_g \sinh(\tilde{b} S \delta)} \quad (\text{Eq. 3})$$

$$R = \frac{1 - R_g [a + b \coth(\tilde{b} S \delta)]}{a - R_g + \tilde{b} \cosh(\tilde{b} S \delta)} \quad (\text{Eq. 4})$$

In this work, equations 3 and 4 have been applied for T_{tot} and R_{tot} respectively, even when collimated components T_{dir} and R_{spec} are not negligible. The error of the applied approximation is calculated below.

Knowing that the relationship between the intrinsic and the extensive scattering and absorption coefficients are [Var97b]:

$$\alpha = \frac{S}{ACP \cdot (1 - FSR)} \quad (\text{Eq. 5}) \quad \beta = \frac{K}{ACP} \quad (\text{Eq. 6})$$

The four flux MLG equations for collimated light beams can be expressed as:

$$\left(\frac{dI_c}{dz} \right)_{MLG} = -(\alpha + \beta) \cdot I_c = -\frac{1}{ACP} \left(\frac{S}{(1 - FSR)} + K \right) \cdot I_c \quad (\text{Eq. 7})$$

$$\left(\frac{dJ_c}{dz} \right)_{MLG} = (\alpha + \beta) \cdot J_c = \frac{1}{ACP} \left(\frac{S}{(1 - FSR)} + K \right) \cdot J_c \quad (\text{Eq. 8})$$

In the same way, the four flux MLG equations for diffuse light beams can be expressed as:

$$\begin{aligned} \left(\frac{dI_d}{dz} \right)_{MLG} &= \\ &- ACP \cdot \beta \cdot I_d - ACP \cdot (1 - FSR_d) \cdot \alpha \cdot I_d + ACP \cdot (1 - FSR_d) \cdot \alpha \cdot J_d + FSR \cdot \alpha \cdot I_c + (1 - FSR_c) \cdot \alpha \cdot J_c = \\ &= -(K + S)I_d + SJ_d + \frac{1}{ACP} \left(\frac{FSR \cdot S}{1 - FSR} \right) \cdot I_c + \frac{1}{ACP} \cdot S \cdot J_c \end{aligned}$$

$$\begin{aligned} \left(\frac{dJ_d}{dz} \right)_{MLG} &= \\ &- ACP \cdot \beta \cdot J_d - ACP \cdot (1 - FSR_d) \cdot \alpha \cdot J_d + ACP \cdot (1 - FSR_d) \cdot \alpha \cdot I_d + FSR \cdot \alpha \cdot J_c + (1 - FSR_c) \cdot \alpha \cdot I_c = \\ &= -(K + S)J_d + SI_d + \frac{1}{ACP} \left(\frac{FSR \cdot S}{1 - FSR} \right) \cdot J_c + \frac{1}{ACP} \cdot S \cdot I_c \end{aligned}$$

However, if the two flux KM equations are used with total light beams (collimated and diffuse) instead of only the diffuse light beams, their equations can be expressed as:

$$\frac{d(I_c + I_d)}{dz} = \left(\frac{dI}{dz} \right)_{KM} = -(S + K) \cdot I + S \cdot J = -(S + K) \cdot (I_c + I_d) + S \cdot (J_c + J_d)$$

$$\frac{d(J_c + J_d)}{dz} = \left(\frac{dJ}{dz} \right)_{KM} = (S + K) \cdot I - S \cdot J = (S + K) \cdot (J_c + J_d) - S \cdot (I_c + I_d)$$

Hence, applying the above two flux KM model instead of the below four flux MLG model in the case of the SPD sample assumes an error. The equations below would not makes the approximation error, but include ACP and FSR unknown parameters.

$$\left(\frac{d(I_c + I_d)}{dz}\right)_{MLG} = -(S + K) \cdot I_d + S \cdot J_d - \frac{1}{ACP} \cdot (S + K) \cdot I_c + \frac{1}{ACP} \cdot S \cdot J_c$$

$$\left(\frac{d(J_c + J_d)}{dz}\right)_{MLG} = (S + K) \cdot J_d - S \cdot I_d + \frac{1}{ACP} \cdot (S + K) \cdot J_c - \frac{1}{ACP} \cdot S \cdot I_c$$

The assumed error of applying the previous equations is the difference between the two flux and the four flux models:

$$\left(\frac{dI}{dz}\right)_{KM} - \left(\frac{d(I_c + I_d)}{dz}\right)_{MLG} = \left(1 - \frac{1}{ACP}\right) \cdot (S + K) \cdot I_c + \left(1 - \frac{1}{ACP}\right) \cdot S \cdot J_c \quad (\text{Eq. 9})$$

$$\left(\frac{dJ}{dz}\right)_{KM} - \left(\frac{d(J_c + J_d)}{dz}\right)_{MLG} = -\left(1 - \frac{1}{ACP}\right) \cdot (S + K) \cdot J_c + \left(1 - \frac{1}{ACP}\right) \cdot S \cdot I_c \quad (\text{Eq. 10})$$

Since two flux KM model considers diffuse illumination, with $ACP=2$ and $FSR=0$, the scattering coefficient S is here completely backscattered. The previous eq. 9 and 10 show the difference of applying two flux KM model with diffuse downwelling I_d and upwelling J_d with respect to total downwelling $I=I_c+I_d$ and upwelling $J=J_c+J_d$. This means that the solution found for S & K is overestimated, i.e., attenuated by scattering and absorption but intensified by scattering of the backward light beam [Lev05].

3. Results and discussion

Predicted transmittance and reflectance is computed backwards for different thicknesses of the internal active layer. Simulated total, diffuse and direct (specular) transmittances and reflectances (T_{tot} , R_{tot} , T_{diff} , R_{diff} , T_{dir} and R_{spec}) were derived from the retrieved scattering and absorption coefficients for different thicknesses in Fig. 6. Once obtained the values of S and K corresponding to the SPD sample, the optical properties have been predicted for a variety of internal layer thicknesses δ of the sample SPD, from 100 μm to 800 μm , in Fig. 6. T_{dir} , and R_{spec} were calculated using r_c and $ext=(\alpha+\beta)$. T_{tot} and R_{tot} were calculated using $\omega^i=r_c$, $\omega^j=r_d$ and R_g . T_{diff} and R_{diff} were calculated from $T_{tot}-T_{dir}$ and $R_{tot}-R_{spec}$. Increments of T_{dir} and R_{spec} are observed when decreasing the thickness (Fig.6-down). For thinner thicknesses than 300 μm (actually the thickness of the SPD sample), a higher contrast of T_{dir} is observed at 200 μm , with higher values for OFF and ON states in the visible wavelength range. However, non desirable increments of R_{spec} are also observed, leading to a more transparent but also more reflective device. Regarding to R_{diff} and T_{diff} (Fig.6-center), there is an appreciable decrement of T_{diff} at 200 μm accompanied with the increment of the R_{diff} , aggravating

the haze of the SPD which could appear as a diffuse mirror-like. R_{tot} and T_{tot} show a clear decrement at the visible range for thicker devices (Fig.6-up).

The optical appearance for each thickness (from 100 to 800 μm) is related to the sRGB color space derived from CIE 1931 Chromaticity coordinates Y_{xy} (being Y the luminance) applied to the direct transmittance in Fig.7 and 8.

Figure 7 shows the CIE 1931 xy chromaticity coordinates from dark OFF state to bleached ON state at the different simulated thicknesses. The thicker the device, the longer distance between xy coordinates at bleached and colored states.

Figure 8 shows the optical appearance of the SPD sample simulated for the different thicknesses. Dark state at simulated 100 microns thickness is not as dark as desired and bleached state at simulated 800 microns is not as bleached as desired. Maximum optical appearance contrast seems to be at thicknesses lower than 400 μm .

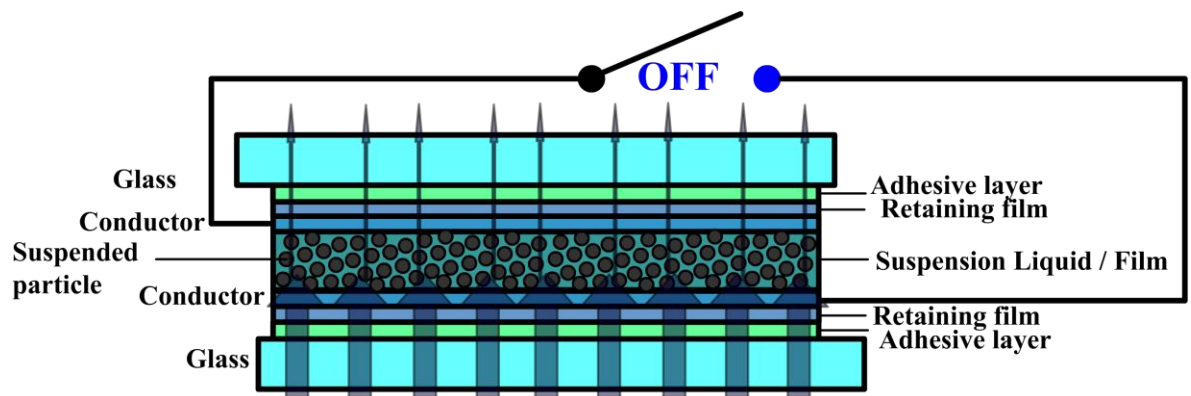
Figure 9 shows thickness dependence of the luminous (up) and solar (down) integrated values of transmittance (left) and reflectance (right) in both OFF and ON states, computed from the expected T_{tot} , T_{dir} and T_{diff} and R_{tot} , R_{spec} and R_{diff} components of Fig. 6 obtained from the calculated S & K coefficients of Fig. 5.

For a better visualization between OFF and ON states, Fig. 10 shows the luminous and solar transmittance (left) and reflectance (right) contrast. Although the maximum ΔT_{tot} and ΔT_{dir} are observed for 200 μm thickness (for both luminous and solar parameters), the undesired high value of $R_{tot,lum}$ for this thickness value (Fig. 10-right-up) of 9.5% and 10.7% for OFF and ON states respectively, can be decreased to 7.9% and 9.7% when increasing the thickness to 300 μm . Another relevant parameter in order to choose the optimum thickness is the haze (Fig. 11), for both transmittance (left) and reflectance (right), as a ratio between the diffuse and the total component.

4. Conclusions

The calculated total and direct transmittance of the SPD decrease with increasing thickness. The highest luminous and solar transmittance contrast is observed at a thickness of 200 μm . However, an increased reflectance is also observed for thicknesses below 300 μm , leading to a more transparent but also more reflective device. The decrease of T_{diff} below 300 μm is accompanied by an increase of R_{diff} , and the reflectance haze can exceed 0.4. Although the maximum ΔT_{tot} and ΔT_{dir} is observed at 200 μm , there exists a tradeoff with reflectance and haze. Luminous transmittance haze can be decreased by using a thinner device, with a slight increment of the reflectance as a drawback. The high value of the simulated luminous transmittance haze at OFF states

is due to the low values of transmittance at this wavelength range when the SPD shows the dark state.



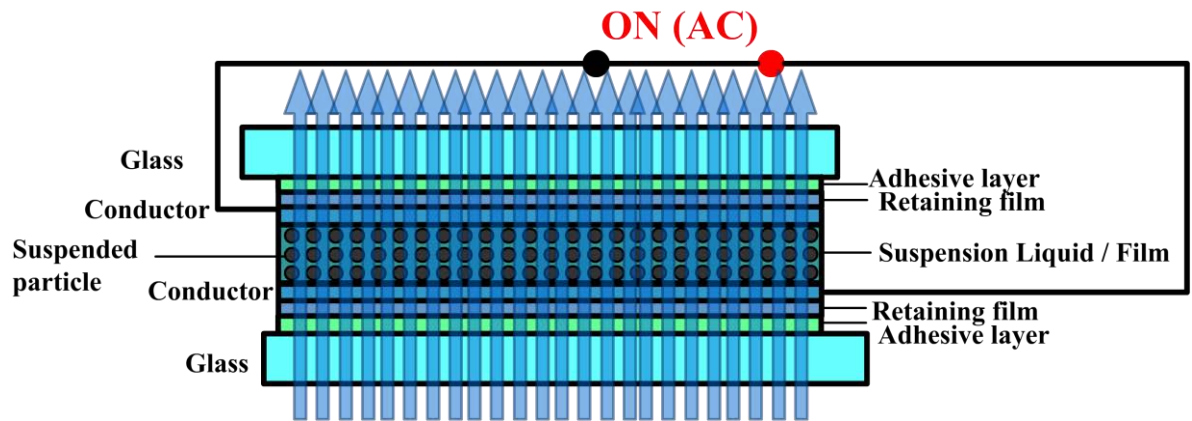


Figure 1: Sandwich structure of a SPD in both OFF and ON states.

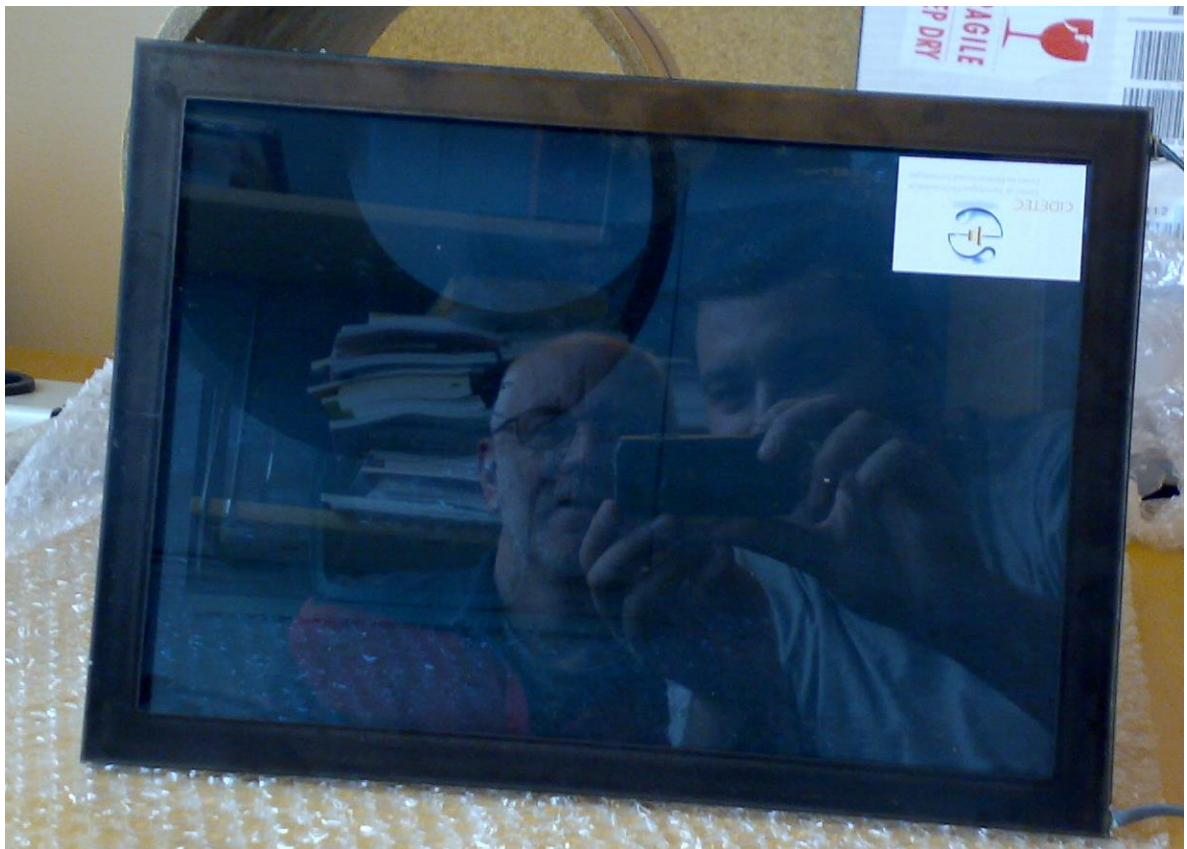
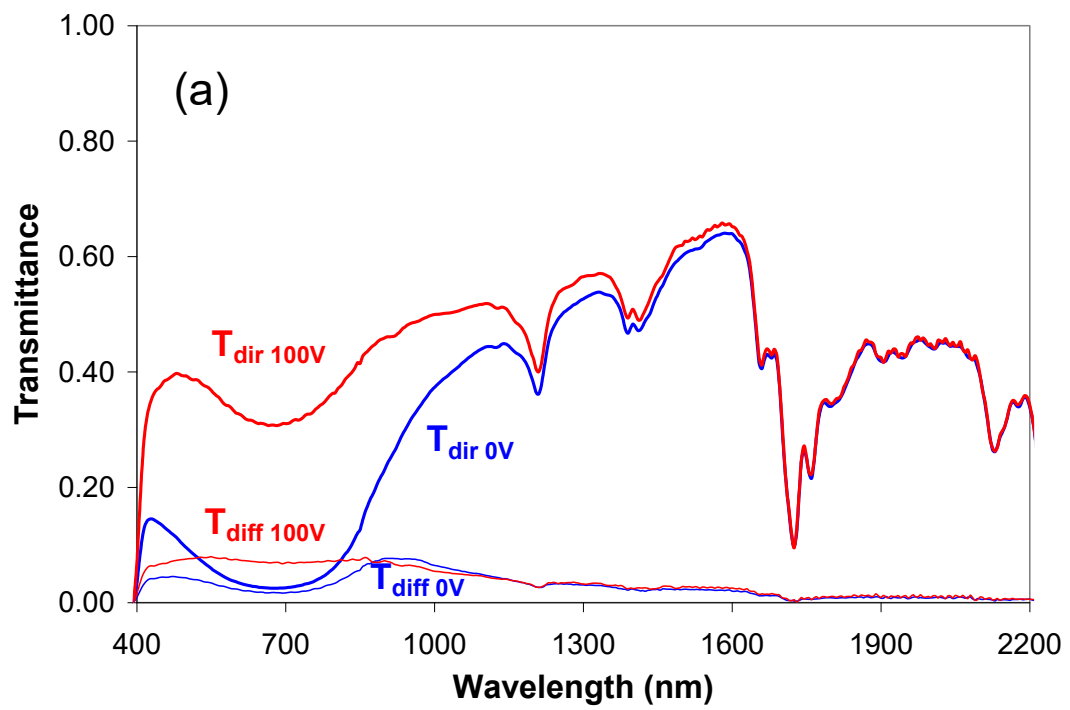




Figure 2: Photograph of the SPD sample for dark and bleached states.

(a) Without applied voltage. (b) With applied voltage.



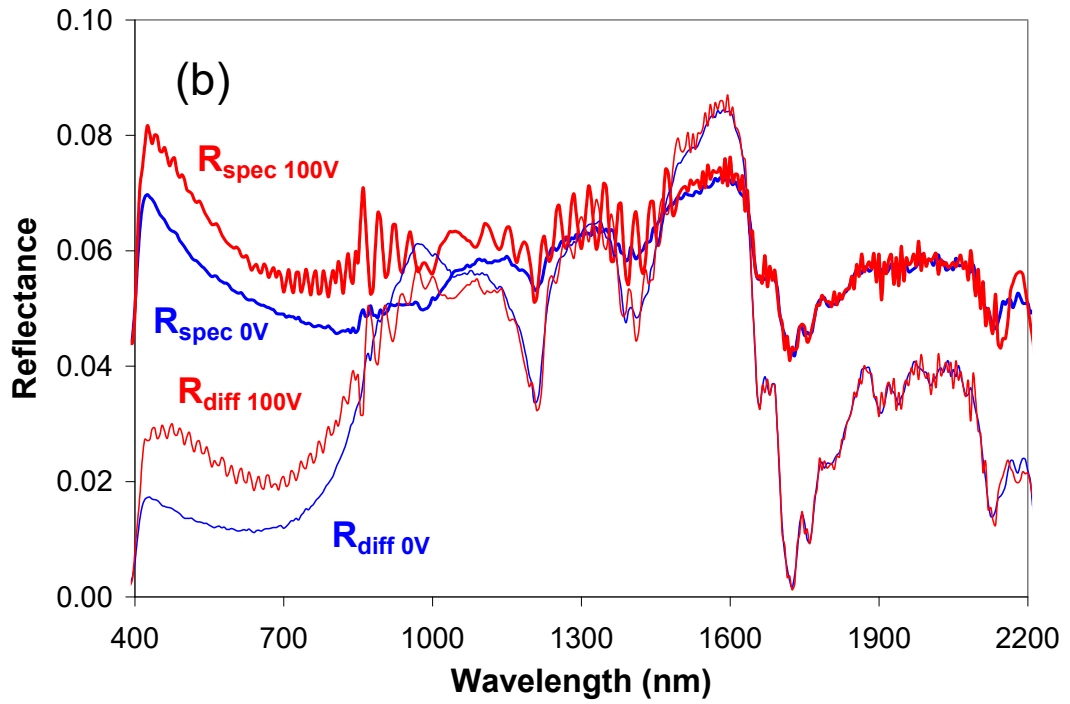
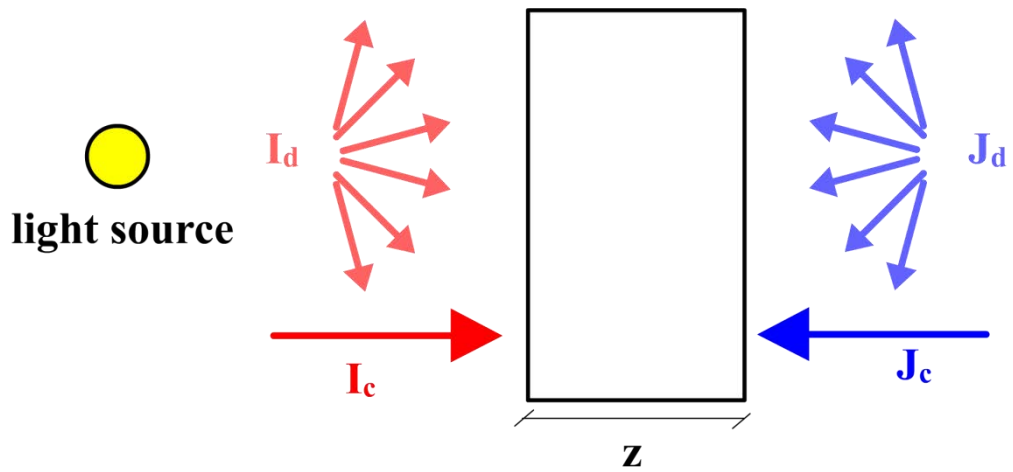


Figure 3: Spectral direct and diffuse transmittance and reflectance for the SPD sample at zero voltage (OFF state) and at $U=100\text{ V}$ (ON state).



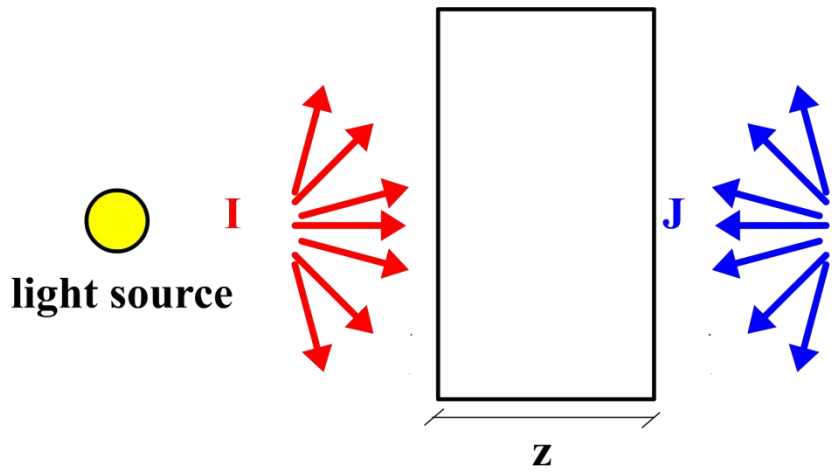


Figure 4: Four-flux model (up) collimated and diffuse light beams.
Two flux model (down) total light beams.

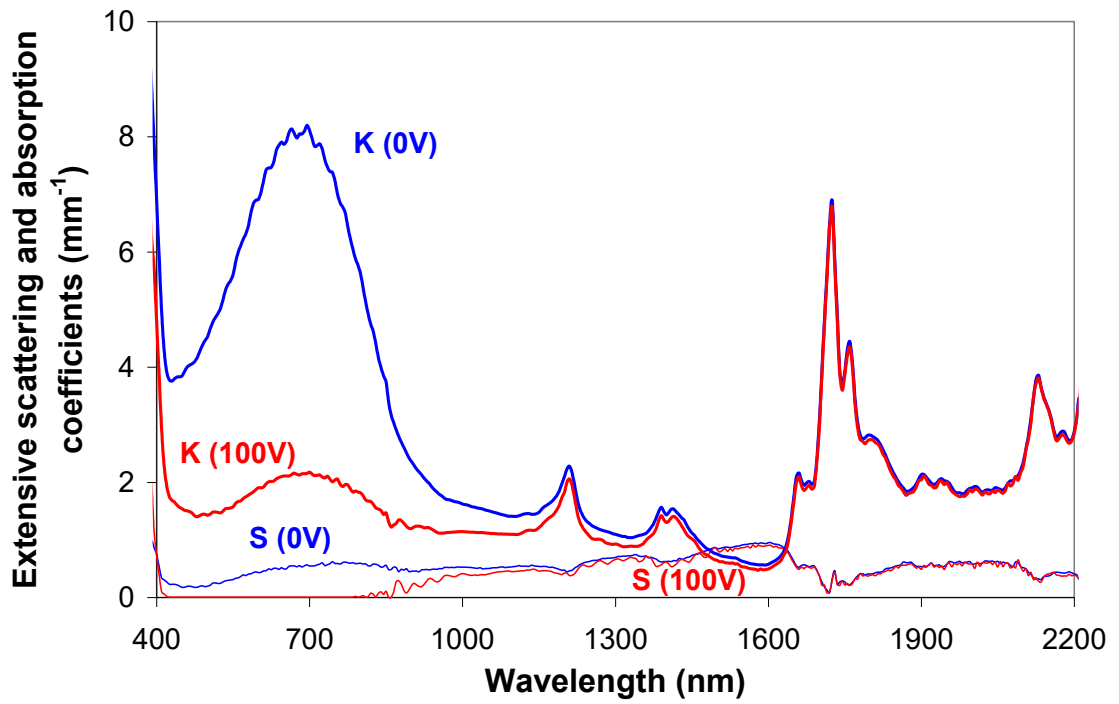
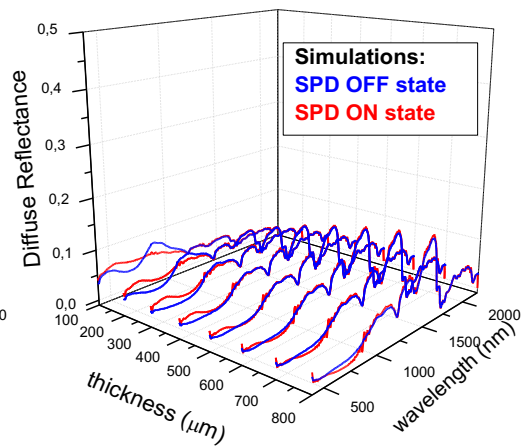
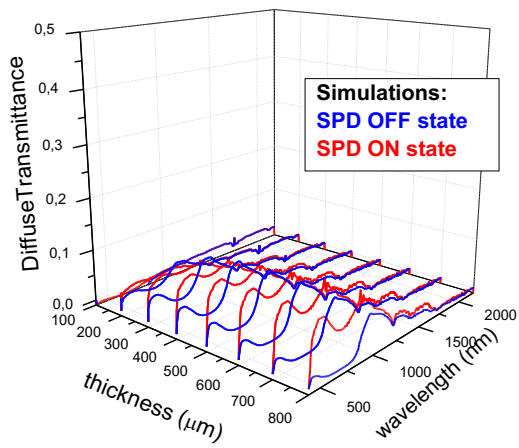
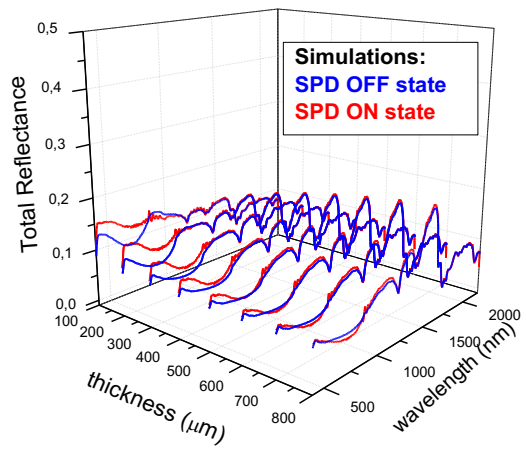
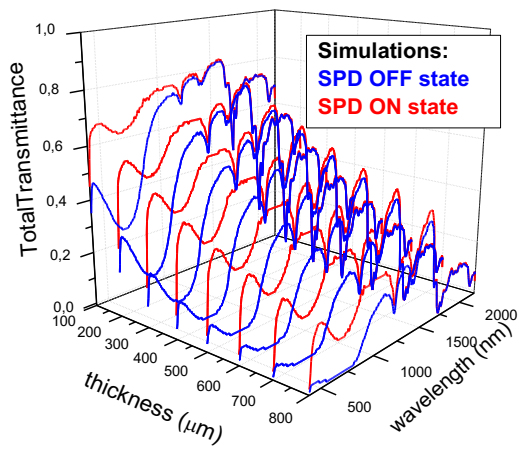


Figure 5: Scattering S and absorption K coefficients for the SPD at zero voltage (OFF state) and for U=100 V (ON' state).



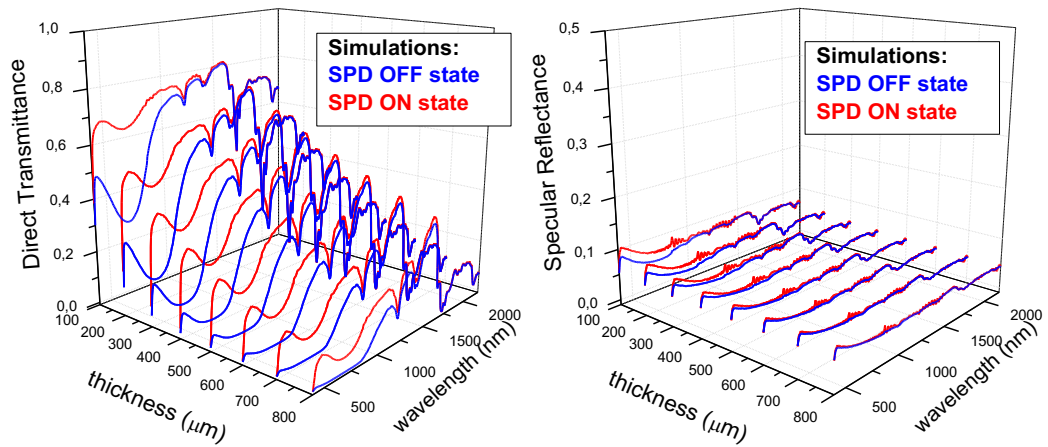


Figure 6: Observed” transmittance (left) & reflectance (right) of sample SPD simulated for different thicknesses. (up) Total T & R, (center) Diffuse T & R and (down) Direct T & Specular R.

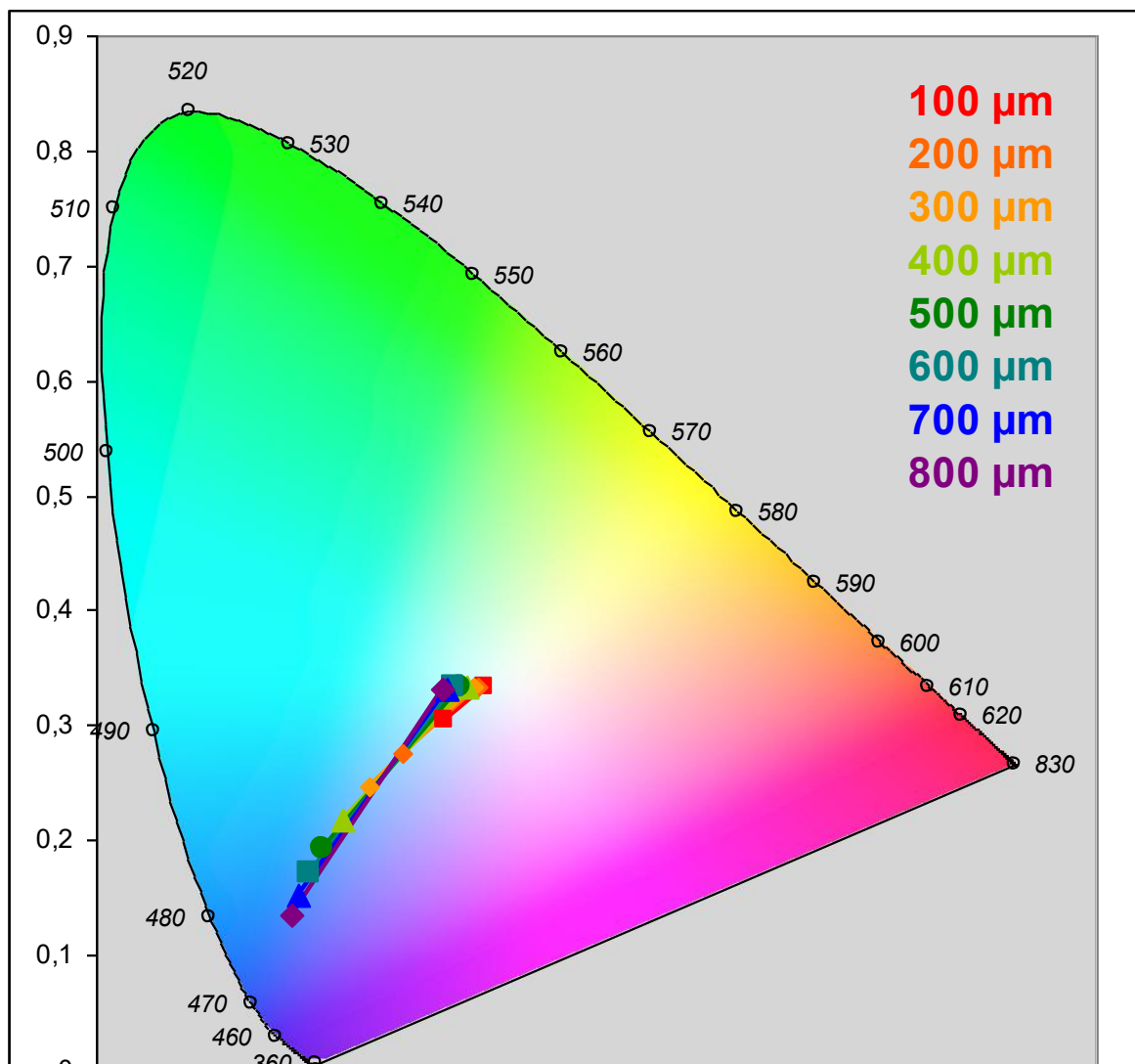


Figure 7: CIE 1931 Chromaticity Coordinates xy of the SPD sample at OFF and ON states for the different simulated thicknesses from 100 to 800 microns.

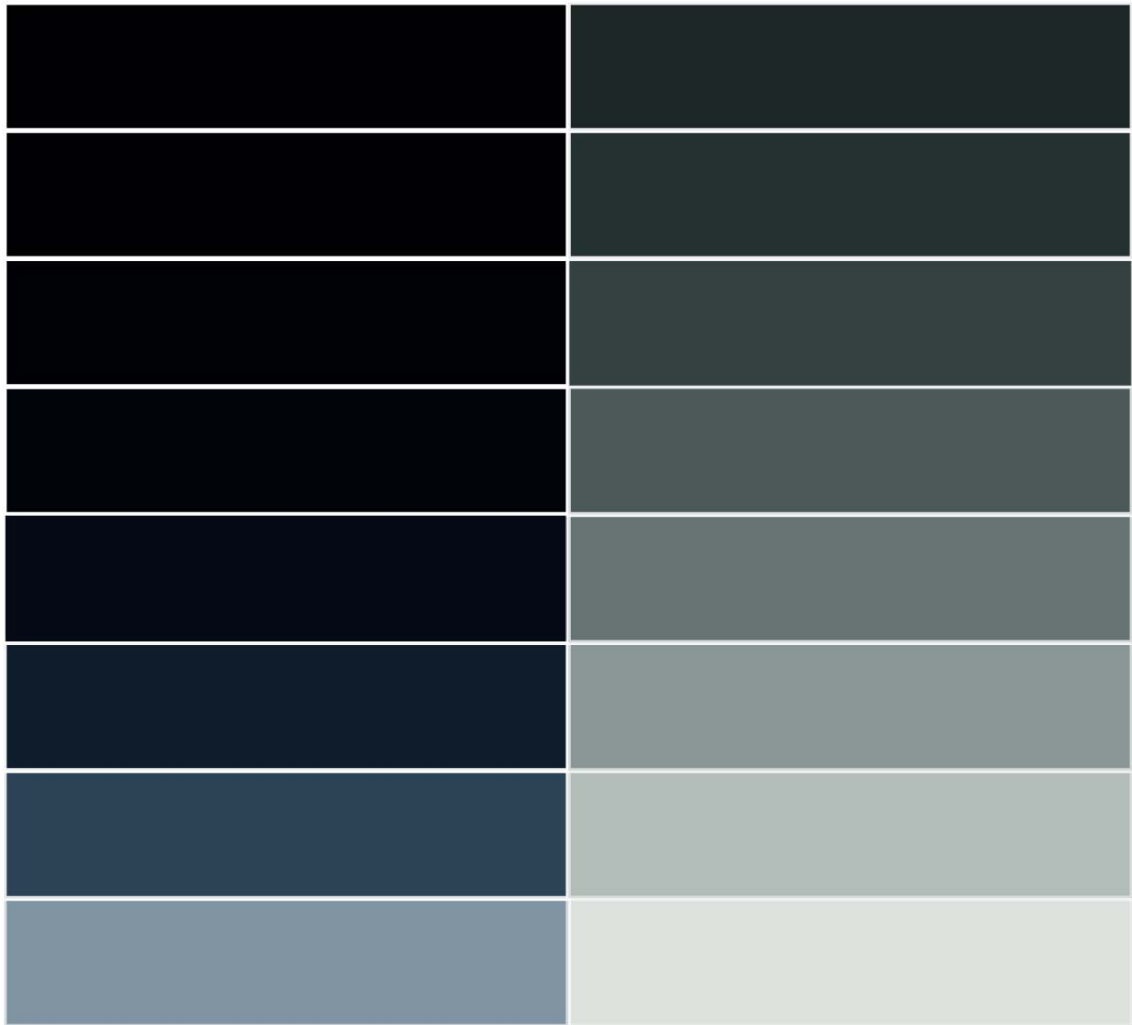


Figure 8: Simulated optical appearance for OFF (left) and ON (right) states of the SPD sample for different thicknesses, from 800 microns (top) to 100 microns (bottom). The constructed thickness was 300 microns.

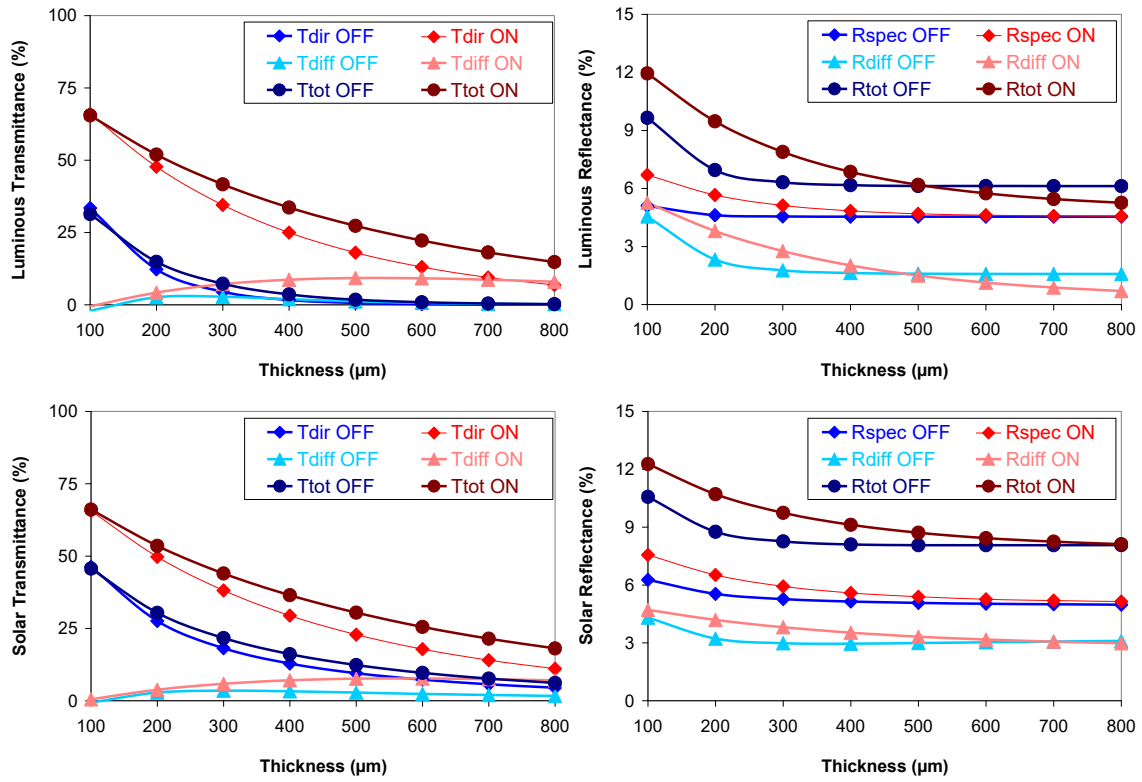


Figure 9: Thickness dependence of luminous (up) and solar (down) of expected transmittances (left) and reflectances (right) derived from the calculated scattering S and absorption K coefficients.

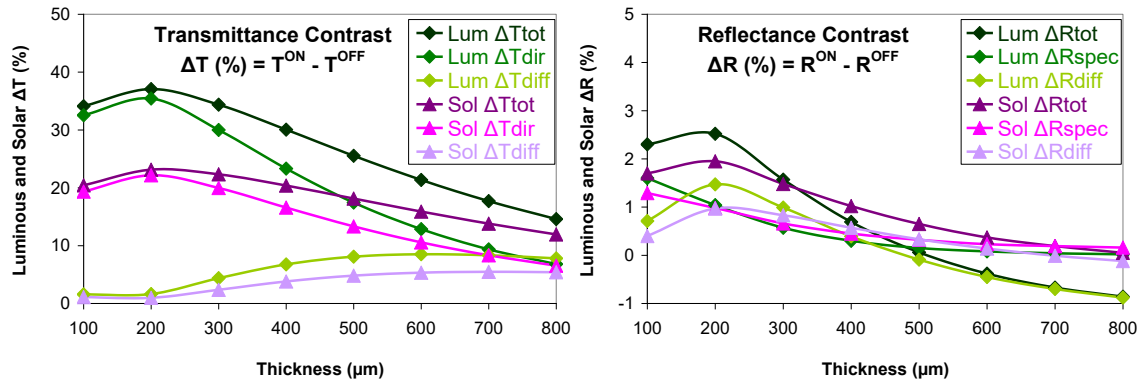


Figure 10: Thickness dependence of luminous and solar transmittance (left) and reflectance (right).

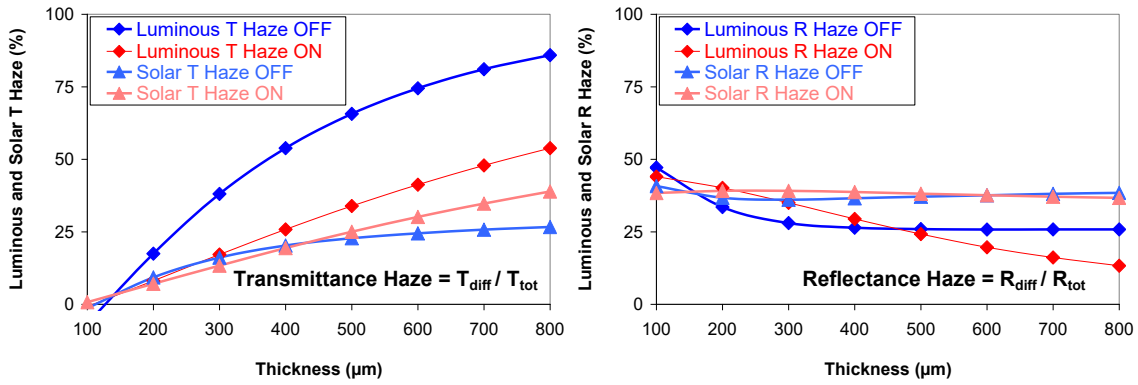


Figure 11: Thickness dependence of luminous and solar transmittance (left) and reflectance (right) hazes.

Acknowledgements

We are grateful to the Prometeo program of Ecuador government and Senescyt (Secretaría Nacional de Educación Superior, Ciencia Tecnología e Innovación). This work was supported by the Comunidad de Madrid (grant No. FACTOTEM2 S2009/ESP-1781).

References

[Bar12] David Barrios, Characterization and applications of new electrochromic devices. Comparison with other electrically controllable transmittance technologies. PhD thesis, Universidad Carlos III de Madrid, 2012.

[Bar13] David Barrios, Ricardo Vergaz, Jose M. Sanchez-Pena, Claes G. Granqvist, Gunnar A. Niklasson, Toward a quantitative model for suspended particle devices: Optical scattering and absorption coefficients, *Solar Energy Materials and Solar Cells* 111 (2013) 115-122.

[Cha02] S. Chakrapani, S.M. Slovak, R.L. Saxe, B. Fanning, SPD films and light valves comprising same, *Research Frontiers-US Patent* 6416827, 2002. See <http://www.patentstorm.us/patents/6416827-description.html>.

[cri] <http://www.cricursa.com>

[Cu02] F. Curiel, W.E. Vargas, R.G. Barrera, "Visible spectral dependence of the scattering and absorption coefficients of pigmented coatings from inversion of diffuse reflectance spectra Applicability conditions of the Kubelka-Munk theory", *Applied Optics* 41 (2002) 5969-5978.

[Gio56] R.G. Giovanelli, "A note on the coefficient of reflection for internally incident diffuse light", *Optica Acta* 3 (3) (1956) 127-130.

[Kah09] B Kahr, J. Freudenthal, S Philips, W Kaminsky, "Herapathite", *Science* 324 (2009) 1407.

[Kno09] K.M. Knowles, "Commentary: Herapathite – the first man-made polarizer", *Philosophical Magazine Letters*, 89 (2000) 745-755.

[Kor69] G. Kortum, *Reflectance Spectroscopy: Principles, Methods, Applications*, Springer, Berlin, 1969

[Kub48] P. Kubelka, "New contributions to the optics of intensely light-scattering materials. Part I.", *Journal of the Optical Society of America* 38 (1948) 448-457.

[Lam94] Carl M. Lampert, —Glazing Materials for Solar and Architectural Applications, International Energy Agency Solar Heating and Cooling Program Task 10-Solar Materials R&D Subtask C-Glazing Materials (1994).

[Lam95] Carl M. Lampert, "Chromogenic Switchable Glazing: Towards the Development of the Smart Window", *Conference Proceedings of WINDOW INNOVATIONS '95* (1995), Toronto (Canada).

[Lam98] Carl M. Lampert, "Smart switchable glazing for solar energy and daylight control", *Solar Energy Materials and Solar Cells* 52 (1998) 207-221.

[Lam03] C.M. Lampert, "Large-area smart glass and integrated photovoltaics", *Solar Energy Materials and Solar Cells* 76 (2003) 489-499.

[Lam04] Carl M. Lampert, "Chromogenic smart materials", *Materials Today* 7 (3) (2004) 28-35.

[Lev05] Ronne Levinson, Paul Berdahl, Hashem Akbari, "Solar spectral optical properties of pigments – Part I: model for deriving scattering and absorption coefficients from transmittance and reflectance measurements", *Solar Energy Materials & Solar Cells* 89 (2005) 319-349.

[LLi09] Lei Liang, Paul Rulis, Bart Kahr, W.Y. Ching, "Theoretical study of the large linear dichroism of herapathite", *Physical Review B* 80, 235132-1-5 (2009).

[MLG84] B. Maheu, J.N. Letoulouzan, G. Gouesbet, "Four-flux models to solve the scattering transfer equation in terms of Lorenz-Mie parameters", *Applied Optics* 23 (1984) 3353- 3362.

[MLG86] B. Maheu and G. Gouesbet, "Four-flux models to solve the scattering transfer equation: special cases", *Applied Optics* 25 (1986) 1122-1128.

[Sau42] J.L. Saunderson, "Calculation of the color of pigmented plastics", *Journal of the Optical Society of America* 32(12) (1942) 727-736.

[RFR] <http://www.refr-spd.com/>

[Rod00] Rodriguez, M. Gomez, J. Ederth, G.A. Niklasson, C.G. Granqvist, "Thickness dependence of the optical properties of sputter deposited Ti oxide films", *Thin Solid Films* 365 (2000) 119-125.

[Roo93] A. Roos, Use of an integrating sphere in solar energy research, *Solar Energy Materials and Solar Cells* 30 (1993) 77-94.

[Sax03] Robert L. Saxe, Barry Fanning, Steven M. Slovak, Robert I. Thompson, Jean Thompson, "Polyhalide particles and light valves comprising same", US patent No. 6517746 (2003).

[Tak97] H. Takeuchi, A. Usuki, N. Tatsuda, H. Tanaka, A. Okada, K. Tojima, *Material Research Society Symposium Proceedings* 424 (1997) 317-322.

[Var97a] William E. Vargas and Gunnar A. Niklasson, "Applicability conditions of the Kubelka-Munk theory", *Applied Optics* 36 (1997) 5580-5586.

[Var97b] William E Vargas and Gunnar A Niklasson, "Forward-scattering ratios and average pathlength parameter in radiative transfer models", *Journal of Physics: Condensed Matter* 9 (1997) 9083-9096.

[Var98] William E. Vargas, "Generalized four-flux radiative transfer model" *Applied Optics* 37 (1998) 2615-2623.

[Var99] William E. Vargas, "Two-flux radiative transfer model under nonisotropic propagating diffuse radiation", *Applied Optics* 38(7) (1999) 1077-1085.

[Ver08] R. Vergaz, J.M.S. Pena, D. Barrios, I. Perez, J.C. Torres, "Electrooptical behaviour and control of a suspended particle device", *Opto-electronic review* 15(3) (2008) 154-158.

[Ver08d] R. Vergaz, J.M.S. Pena, D. Barrios, C. Vazquez, P. Contreras-Lallana, "Modelling and electro-optical testing of suspended particle devices", *Solar Energy Materials and Solar Cells* 92 (2008) 1483-1487.

Figure Captions

Fig. 1: Sandwich structure of a SPD in both OFF and ON states.

Fig. 2: Photograph of the SPD sample for dark and bleached states. (a) Without applied voltage. (b) With applied voltage.

Fig. 3: Spectral direct and diffuse transmittance and reflectance for the SPD sample at zero voltage (OFF state) and at $U=100$ V (ON state).

Fig. 4: Four-flux model (up) collimated and diffuse light beams. Two flux model (down) total light beams.

Fig. 5: Scattering S and absorption K coefficients for the SPD at zero voltage (OFF state) and for $U=100$ V (ON state).

Fig. 6: Observed" transmittance (left) & reflectance (right) of sample SPD simulated for different thicknesses. (up) Total T & R , (center) Diffuse T & R and (down) Direct T & Specular R .

Fig. 7: CIE 1931 Chromaticity Coordinates xy of the SPD sample at OFF and ON states for the different simulated thicknesses from 100 to 800 microns.

Fig. 8: Simulated optical appearance for OFF (left) and ON (right) states of the SPD sample for different thicknesses, from 800 microns (top) to 100 microns (bottom). The constructed thickness was 300 microns.

Fig. 9: Thickness dependence of luminous (up) and solar (down) of expected transmittances (left) and reflectances (right) derived from the calculated scattering S and absorption K coefficients.

Fig. 10: Thickness dependence of luminous and solar transmittance (left) and reflectance (right).

Fig. 11: Thickness dependence of luminous and solar transmittance (left) and reflectance (right) hazes.